PHYSICAL REVIEW A **87**, 054701 (2013)

Experimental study of the formation of ultracold RbCs molecules by short-range photoassociation

A. Fioretti and C. Gabbanini[*]
Istituto Nazionale di Ottica, INO-CNR, U. O. S. Pisa “Adriano Gozzini” Via Moruzzi 1, 56124 Pisa, Italy

(Received 25 February 2013; published 17 May 2013)

We have experimentally studied the formation of ultracold RbCs molecules by photoassociation at short internuclear range followed by spontaneous emission. The observation of new excited levels with respect to our previous work [Gabbanini and Dulieu, Phys. Chem. Chem. Phys. **13**, 18905 (2011)] on both sides of the $\mathrm{Rb}(5S_{1/2})+\mathrm{Cs}(6P_{3/2})$ dissociation limit gives information on the state responsible for molecule formation. The molecules are mainly formed in deeply bound levels of the electronic triplet ground state. The observed photoassociation transitions present differences in terms of saturation.

DOI: 10.1103/PhysRevA.87.054701 PACS number(s): 34.50.Cx, 37.10.Mn, 33.20.Ea

Following important advances in manipulating the internal and external degrees of freedom of molecules, many applications of ultracold molecules have been proposed and in some cases already demonstrated. The applications span different fields including fundamental tests in physics, molecular clocks, molecular spectroscopy, ultracold reactions, controlled photochemistry, and quantum computation [1]. In particular, cold polar molecules are interesting for the properties related to their permanent electric dipole moment. Polar molecules can be manipulated by external electric fields, allowing for the control of elementary chemical reactions at low temperatures. Heteronuclear alkali-metal molecules in the lowest vibrational level of their ground state $X\,^1\Sigma^+$ possess a permanent electric dipole moment from a half to a few debye [2] that determines long-range anisotropic dipole-dipole interactions in the presence of an external polarizing electric field.

One of the most successful techniques able to obtain ultracold molecules is photoassociation (PA) of laser cooled atoms followed by stabilization via spontaneous emission [3,4]. The process produces molecules that are generally distributed in high-lying rovibrational levels of the ground singlet or lowest metastable triplet state. These molecules have a weakly polar character but represent a starting point for a further manipulation that can transfer them into the lowest vibrational level $v=0$. This can be achieved by a coherent optical process, using the stimulated Raman adiabatic passage process [5,6] or, with lower efficiency, by an incoherent process, as done for the transfer of the vibrational population in the $v=0$ level of the RbCs ground state [7]. A further possibility involves the cooling of the vibrational and rotational degree of freedom utilizing a properly shaped laser [8–10]. All these methods require detailed insights on molecular spectra and the knowledge of the rovibrational distribution of the created cold molecules.

In a previous work we reported the formation of ultracold RbCs molecules by PA and subsequent stabilization in a double species magneto-optical trap (MOT) [11]. We proposed an interpretation relying on PA at short internuclear distance and predicted that ultracold RbCs molecules can be formed in deeply bound vibrational levels (including $v=0$) of the lowest electronic triplet state and of the ground singlet state [12]. Here we report the observation of other excited levels, on both sides of the $\mathrm{Rb}(5S_{1/2})+\mathrm{Cs}(6P_{3/2})$ dissociation limit, that gives information on the state responsible for molecule formation.

The experiment is done in a double species magneto-optical trap (MOT). The details of the MOTs setup can be found in Refs. [11,12]. The MOT captures about 10^7 atoms of both Cs and ^{85}Rb species with densities of a few 10^{10} cm^{-3} and a temperature in the 100–200 μK range.

The colliding Rb and Cs atoms are photoassociated by a tapered amplifier that is injected by a distributed-feedback (DFB) diode laser. Thanks to its large bandwidth, the tapered amplifier can be injected for all the tuning range of the DFB diode laser, that, by changing its current and temperature, exceeds thirty wave numbers. Outside this tuning range the tapered amplifier is injected by a homemade external cavity diode laser (ECDL). A light power up to 0.6 W is available to be focused on the trapped sample. The absolute PA laser frequency is measured by a wave meter, while a Fabry-Pérot interferometer monitors the frequency scan. The FP interferometer can be also used to frequency lock the DFB laser or the ECDL.

The molecules are resonantly ionized by a laser pulse, given by a dye laser pumped by the second harmonics of a Nd:YAG laser (20 Hz repetition rate and 10 ns time width). The pulsed beam, with typical energy of 1 mJ, is softly focused to the cold sample. The pulsed laser is sent after the repumping lasers of the double MOT have been turned off for a few ms, making momentary dark spot MOTs. This has the double advantage of an initial increase of the atomic densities and a decrease of the collisional losses (both single species and interspecies) that are stronger with atoms in the excited states. After the laser pulse the produced atomic and molecular ions are repelled by a grid, separated by time of flight, and detected by a microchannel plate. The ion signals are then recorded by gated integrators.

In a previous work [11] we observed that, for a few particular frequencies of the PA laser below the $\mathrm{Rb}(5S_{1/2})+\mathrm{Cs}(6P_{3/2})$ dissociation limit, stable RbCs molecules are created by radiative stabilization. The transitions have been identified as different rotational levels of a single vibrational level excited by PA. The large value of the corresponding rotational constant indicates that the PA process acts at short range. The two arguments that the lines do not exhibit any significant hyperfine structure and that the rotational progression starts with $J=0$ determine that the excited

---

[*] carlo.gabbanini@ino.it

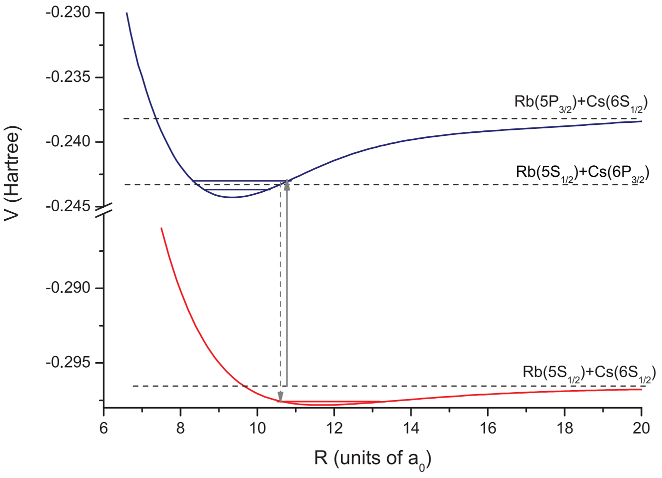

FIG. 1. (Color online) Formation process of RbCs molecules: photoassociation to the (5)0^+ state and radiative stabilization to the a $^3\Sigma^+$ state.

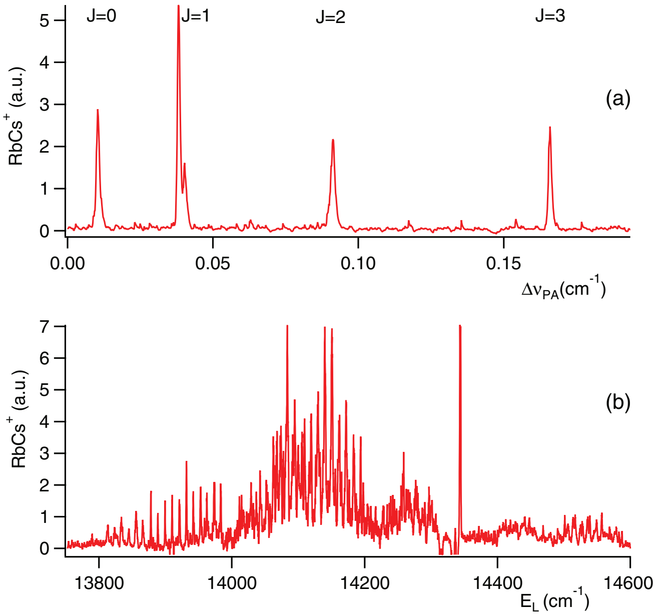

FIG. 2. (Color online) (a) Rotational structure of the PA line at 11 751.157 cm^{-1}; (b) REMPI spectrum of produced RbCs molecules. The peaks near 14 330 cm^{-1} are due to atomic ionization.

electronic state must have a zero value of the projection of the total electronic angular momentum on the molecular axis. A subsequent theoretical investigation [12] including spin-orbit interaction explained the PA process as excitation at short internuclear distance of a vibrational level of the (5)0^+ or (4)0^- electronic states [in Hund's case (c) notation] that originate from the (2)$\,^3\Pi$ state [in Hund's case (a)], and correlated to the Rb$(5P_{3/2})$ + Cs$(6S_{1/2})$ and Rb$(5P_{1/2})$ + Cs$(6S_{1/2})$ dissociation limit, respectively, as shown in Fig. 1. The computed vibrational distribution of the RbCs molecules indicates that they are mainly created in deeply bound vibrational states of the lowest triplet state $a\,^3\Sigma^+$, and possibly with a fraction of molecules in the lowest vibrational levels of the $X\,^1\Sigma^+$ ground state [only if the (5)0^+ state is populated].

Here we report other PA lines that form stable RbCs molecules by radiative stabilization. The lines are positioned on both sides of the Rb$(5S_{1/2})$ + Cs$(6P_{3/2})$ dissociation limit. This is one of the few cases where molecule formation is observed following blue detuned photoassociation [13]. The observed lines correspond to rotational progressions of three additional vibrational levels. The transition frequencies to the $J = 0$ levels are given in Table I. The rotational progression of one of these lines is shown in Fig. 2(a). The strongest line $J = 1$ is split into two components due to the Stark effect induced by the static electric field used for ion extraction.

Both the rotational structure and the rotational constant are consistent with those of the vibrational level observed in Ref. [11], whose constant is now measured slightly different from [11] thanks to the observation of an additional rotational transition ($J = 3$); it is also in agreement with the more precise measurement of Ref. [14]. We also checked that the resonance-enhanced multiphoton ionization (REMPI) spectra of the produced RbCs molecules present the same spectral lines. One of the spectra is shown in Fig. 2(b). The spectral structure is due to the (3)$\,^3\Pi \leftarrow a\,^3\Sigma^+$ and (4)$\,^3\Sigma^+ \leftarrow a\,^3\Sigma^+$

TABLE I. Experimental energies E_{expt} of the observed vibrational states v (for rotational transition $J = 0$) of the (5)0^+ state together with the fitted values E_{fit}, the computed energies E_{theor} [12], the measured rotational constants B_v (cm^{-1}), and the calculated Franck-Condon factors (FC) of the first twelve vibrational levels of the (5)0^+ state with the continuum.

v	E_{expt} (cm^{-1})	E_{fit} (cm^{-1})	E_{theor} (cm^{-1})	B_v (cm^{-1})	FC
0		11 488.156	11 472.39		1.1×10^{-6}
1		11 519.472	11 503.93		4.2×10^{-6}
2		11 550.265	11 535.21		5.3×10^{-6}
3		11 580.534	11 566.21		1.5×10^{-6}
4		11 610.280	11 596.94		4.0×10^{-7}
5		11 639.503	11 627.39		3.3×10^{-6}
6	11 668.203(15)	11 668.202	11 657.56	0.013 3(6)	1.7×10^{-6}
7		11 696.378	11 687.44		2.0×10^{-7}
8	11 724.044(15)	11 724.030	11 717.02	0.013 1(6)	2.9×10^{-6}
9	11 751.157(15)	11 751.160	11 746.21	0.013 0(6)	1.3×10^{-6}
10		11 777.765	11 775.30		3.7×10^{-7}
11	11 803.853(15)	11 803.848	11 803.98	0.012 9(6)	2.8×10^{-6}

molecular bands; the interpretation of the spectra will be published elsewhere. From the rotational structure and the detection spectra we can conclude that the observed PA levels belong to the same electronic state. The comparison with the computations (Fig. 6 of Ref. [12]) suggests that the state responsible for molecule formation is the $(5)0^+$ state. This interpretation is consistent with that of Ref. [14], where just one level was observed and the analysis was based on the accurate value of the rotational constant. In this energy range, as shown in Fig. 5(a) of Ref. [12], there are two 0^+ series, one with small rotational constant and main weight on the $(3)\,{}^1\Sigma^+$ state and the other one with large rotational constant and main weight on the $(2)\,{}^3\Pi$ state, that matches much better our observations. The experimental measurements are in reasonable agreement with the coupled-state calculations both for line positions, that in the investigated range differ by just a few cm^{-1}, and for line intensities, as we observed just the lines with the largest Franck-Condon factors. The experimental signal-to-noise ratio is about 20 for the strongest line; therefore, it is sufficient that the effective FCs of the weak lines are a factor of 2 lower that the computed ones to make them hardly detectable. Other levels having high FC factors could be observed as well, but lie outside the tuning range of our PA laser system.

The observed vibrational progression can be well fitted by a simple anharmonic potential as $E(v) = T_e + \hbar\omega_e(v + \frac{1}{2}) - \omega_e x_e(v + \frac{1}{2})^2$.

By considering the observed levels as the $v = 6,8,9,11$ vibrational states of the $(5)0^+$ series with the main weight on the $(2)\,{}^3\Pi$ state, we can determine the constants $\omega_e = 31.84(4)$ cm^{-1}, $\omega_e x_e = 0.262(2)$ cm^{-1}, and $T_e = 11\,472.30(18)$ cm^{-1}. The energy-level positions derived from the fit are reported in Table I.

The PA rate has been the subject of several theoretical studies [15–17]. The rate is predicted to increase linearly with intensity at low intensities, while at higher intensities some mechanisms may cause saturation of the PA rate, the most important being the quantum-mechanical unitarity limit on the rate of atomic collisions. Following a first experiment that investigated PA at high intensity in a Bose-Einstein condensate [18], the saturation of the PA rate has been observed both in a quantum degenerate gas [19] and in a MOT [20]. The observations concern red detuned photoassociation. If PA occurs on the blue side of an atomic dissociation limit, the PA laser can couple colliding atoms to a repulsive potential, preventing the atoms from reaching the short internuclear range. This phenomenon has been studied and used as a “blue shielding” of atomic collisions at low temperature [21].

We have investigated the saturation behavior of three PA resonances that produce ultracold molecules after radiative stabilization. The measurements have been done on the strongest rotational component $J = 1$ by changing the PA laser intensity I_L with neutral filters, tuning the PA laser to the maximum signal for each intensity to compensate eventual line shift. The results are shown in Fig. 3.

The data are fitted by a function $R(I_L) = cI_L/(I_L + I_S)^2$, that comes from the theoretical model of PA in strong laser field [17], where I_S is the saturation intensity and c a constant.

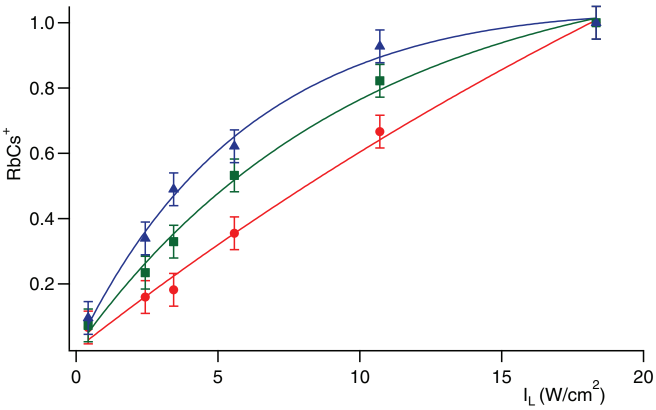

FIG. 3. (Color online) Normalized RbCs^+ ion signal as a function of the PA laser intensity for three PA transitions: circles: line at $11\,724.044$ cm^{-1}; triangles: line at $11\,751.157$ cm^{-1}; squares: line at $11\,803.853$ cm^{-1}.

The PA line on the red side of the asymptote shows faint saturation for the available intensity range. The fit gives a saturation intensity of 163 W/cm^2, larger but of the same order of that measured in Ref. [14] for the same line (102 W/cm^2). The two blue PA lines show stronger evidence of saturation. In particular, the line closer to the dissociation limit presents a stronger saturation ($I_S = 23$ W/cm^2 compared with $I_S = 38$ W/cm^2 for the other blue line). We can exclude that the dipolar antitrapping effect of the blue light can play a role, as the potential height associated with the blue line closest to the $\text{Rb}(5S_{1/2}) + \text{Cs}(6P_{3/2})$ dissociation limit is for cesium atoms of the order of 2 μK, well below the trapping potential of the MOT. As the lines investigated have similar Franck-Condon factors, we hypothesize that the saturation is related to the coupling to a repulsive state on the blue side of the $\text{Rb}(5S_{1/2}) + \text{Cs}(6P_{3/2})$ dissociation limit that lowers the flux at short internuclear range.

To conclude, we have investigated the formation of ultracold RbCs molecules by photoassociation near the $\text{Rb}(5S_{1/2}) + \text{Cs}(6P_{3/2})$ dissociation limit. The experimental observations together with the theoretical analysis done in Ref. [12] suggest that the PA process occurs at short internuclear range through the $(5)0^+$ electronic state that originates from the $(2)\,{}^3\Pi$ state. From this state the radiative stabilization forms molecules mainly in deeply bound levels of the electronic triplet ground state. A fraction of the excited molecules should also decay in the lowest vibrational levels of the $X\,{}^1\Sigma^+$ ground state. This will be the subject of a future investigation, with the perspective to transfer the whole population to the ground rovibrational state. The observed photoassociation transitions that are on opposite sides of the $\text{Rb}(5S_{1/2}) + \text{Cs}(6P_{3/2})$ dissociation limit display different behavior in terms of saturation of the molecular formation rate, that we interpret as a shielding of the atomic flux at short internuclear range for the blue detuned lines.

The author wishes to thank N. Bouloufa-Maafa and O. Dulieu for kindly providing the theoretical calculations and F. Pardini for technical support.

[1] R. V. Krems, W. C. Stwalley, and B. Friedrich, *Cold Molecules: Theory, Experiment, Applications* (CRC Press, Boca Raton, FL, 2009).
[2] M. Aymar and O. Dulieu, J. Chem. Phys. **122**, 204302 (2005).
[3] O. Dulieu and C. Gabbanini, Rep. Prog. Phys. **72**, 086401 (2009).
[4] J. Ulmanis, J. Deiglmayr, M. Repp, R. Westerand, and M. Weidemuller, Chem. Rev. **112**, 4890 (2012).
[5] F. Lang, K. Winkler, C. Strauss, R. Grimm, and J. Hecker Denschlag, Phys. Rev. Lett. **101**, 133005 (2008).
[6] K. Aikawa, D. Akamatsu, M. Hayashi, K. Oasa, J. Kobayashi, P. Naidon, T. Kishimoto, M. Ueda, and S. Inouye, Phys. Rev. Lett. **105**, 203001 (2010).
[7] J. M. Sage, S. Sainis, T. Bergeman, and D. DeMille, Phys. Rev. Lett. **94**, 203001 (2005).
[8] M. Viteau, A. Chotia, M. Allegrini, N. Bouloufa, O. Dulieu, D. Comparat, and P. Pillet, Science **321**, 232 (2008).
[9] A. Wakim, P. Zabawa, M. Haruza, and N. P. Bigelow, Opt. Express **20**, 16083 (2012).
[10] I. Manai, R. Horchani, H. Lignier, P. Pillet, D. Comparat, A. Fioretti, and M. Allegrini, Phys. Rev. Lett. **109**, 183001 (2012).
[11] C. Gabbanini and O. Dulieu, Phys. Chem. Chem. Phys. **13**, 18905 (2011).
[12] N. Bouloufa-Maafa, M. Aymar, O. Dulieu, and C. Gabbanini, Laser Phys. **22**, 1502 (2012).
[13] M. A. Bellos, R. Carollo, D. Rahmlow, J. Banerjee, E. E. Eyler, P. L. Gould, and W. C. Stwalley, Phys. Rev. A **86**, 033407 (2012).
[14] Z. Ji, H. Zhang, J. Hu, J. Yuan, Y. Yang, Y. Zhao, J. Ma, L. Wang, L. Xiao, and S. Jia, Phys. Rev. A **85**, 013401 (2012).
[15] R. Napolitano, J. Weiner, C. J. Williams, and P. S. Julienne, Phys. Rev. Lett. **73**, 1352 (1994).
[16] P. Pillet, A. Crubellier, A. Bleton, O. Dulieu, P. Nosbaum, I. Mourachko, and F. Masnou-Seeuws, J. Phys. B **30**, 2801 (1997).
[17] J. L. Bohn and P. S. Julienne, Phys. Rev. A **60**, 414 (1999).
[18] C. McKenzie, J. Hecker Denschlag, H. Haffner, A. Browaeys, L. E. E. de Araujo, F. K. Fatemi, K. M. Jones, J. E. Simsarian, D. Cho, A. Simoni, E. Tiesinga, P. S. Julienne, K. Helmerson, P. D. Lett, S. L. Rolston, and W. D. Phillips, Phys. Rev. Lett. **88**, 120403 (2002).
[19] I. D. Prodan, M. Pichler, M. Junker, R. G. Hulet, and J. L. Bohn, Phys. Rev. Lett. **91**, 080402 (2003).
[20] U. Schloder, C. Silber, T. Deuschle, and C. Zimmermann, Phys. Rev. A **66**, 061403 (2002).
[21] V. Sanchez-Villicana, S. D. Gensemer, K. Y. N. Tan, A. Kumarakrishnan, T. P. Dinneen, W. Suptitz, and P. L. Gould, Phys. Rev. Lett. **74**, 4619 (1995).